Author(s): Rämö, J.; Välimäki, V.

Title: Optimizing a High-Order Graphic Equalizer for Audio Processing

Year: 2014

Version: Post print

Please cite the original version:

J. Rämö and V. Välimäki. Optimizing a High-Order Graphic Equalizer for Audio Processing. IEEE Signal Processing Letters, Vol. 21, No. 3, pp. 301-305, March 2014. DOI: 10.1109/LSP.2014.2301557

Optimizing a High-Order Graphic Equalizer for Audio Processing

Jussi Rämö* and Vesa Välimäki, *Senior Member, IEEE*

***Abstract*—A high-order graphic equalizer has the advantage that the gain in one band is highly independent of the gains in the adjacent bands. However, all practical filters have transition bands, which interact with the adjacent bands and create errors in the desired magnitude response. This letter proposes a filter optimization algorithm for a high-order graphic equalizer, which minimizes the errors in the transition bands by iteratively optimizing the orders of adjacent band filters. The optimization of the filter order affects the shape of the transition band, thus enabling the search for the optimum shape relative to the adjacent filter. The optimization is done offline, and during filtering only the gains of the band filters are altered. In an example case, the proposed method was able to meet the given peak-error limitations of ± 2 dB, when the total order of the graphical equalizer was 328, whereas the non-optimized filter could not meet the requirements even when the total order was raised to 672. Optimized high-order graphical equalizers can be widely used in audio signal processing applications.**

***Index Terms*—Acoustic signal processing, audio systems, digital signal processing, equalizers, music.**

I. Introduction

EQUALIZERS were originally used to make the frequency response of a telephone or audio system flat. However, nowadays in music audio processing, the objective of equalizing is usually not to flatten the response, but to enhance signal characteristics or to meet other desired requirements, e.g., strengthen the quarter wavelength resonance of the ear canal in headphone listening. Equalizers are widely used, e.g., in music production and in live sound reproduction to control the timbral balance of the music. Equalizers are also used to attenuate unwanted sounds, such as the acoustic feedback occurring when a microphone is close to a loudspeaker, like in live concerts and in hearing aids.

The two most common equalizers are the parametric [1], [2], [3] and the graphic equalizer [4], [5]. Parametric equalizers allow the user to control the gain, center frequency, and bandwidth of the equalizer filters, while graphic equalizers typically have a preset center frequency and bandwidth, and the only user-adjustable control is the gain. The gain is typically controlled using a set of sliders, whose knob positions draw the magnitude response of the equalizer as the user adjusts them.

Many digital equalizers are based on analog filters, whose analog transfer functions are transformed into the digital domain [6], e.g., by using a bilinear transform [7]. However, equalizer filters can also be designed directly in the digital domain [2], [3], [8]. The basic building block of an equalizer is usually a second-order IIR biquad filter, but also designs based on parallel allpass filters [9] and multirate filter banks have been proposed [10], [11]. A well-known tunable digital second-order equalizer filter was originally presented by Regalia and Mitra [1] and later improved by Zölzer and Boltze [12] as well as by Fontana and Karjalainen [13].

The authors are with Aalto University School of Electrical Engineering, Department of Signal Processing and Acoustics, P.O. Box 13000, FI-00076 AALTO, Espoo, Finland (e-mail: jussi.ramo@aalto.fi; vesa.valimaki@aalto.fi).

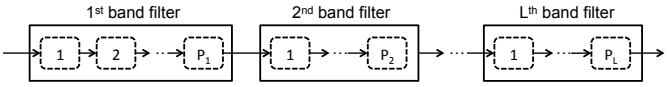

Fig. 1. Graphic equalizer having L band filters (solid blocks) consisting of cascaded fourth-order sections (dashed blocks).

However, low-order graphic equalizers, such as those based on second-order filters, suffer from filter overlapping, especially at transition bands, which deteriorates the overall response of the equalizer. The ideal case would be to have completely independent gain control for each band of the equalizer, but a realizable peak or notch filter always has transition bands [14] which determine how it interacts with the adjacent filters. By increasing the filter order, the errors at the transition bands typically become smaller and the overall magnitude response of the equalizer improves. We have previously utilized a high-order graphic equalizer in auditory masking-related research [15], [16] by attenuating and emphasizing individual critical bands, where the need for individual control over each critical band demands a high-order equalizer.

The filter structure discussed in this letter is based on a recursive high-order equalizer design proposed by Orfanidis [17]. Holters and Zölzer [4] presented a graphic equalizer design which uses cascaded fourth-order sections that produce minimum-phase behaviour. The proposed optimization further improves the overall high-order equalizer response at the transition bands. The errors in the transition bands emerge when the adjacent filters have differently shaped, asymmetric, slopes. The order of the filter affects the shape of the filter slope, which makes the iterative search of the optimum shape possible when comparing adjacent band filters.

The letter is organized as follows. Section II describes the high-order equalizer design, Section III introduces the filter-order optimization algorithm, Section IV presents design examples and compares them to non-optimized graphic equalizers, and Section V concludes the paper.

II. Graphic Equalizer Design

The graphic equalizer consists of band filters, where every filter comprises cascaded fourth-order sections, as shown in

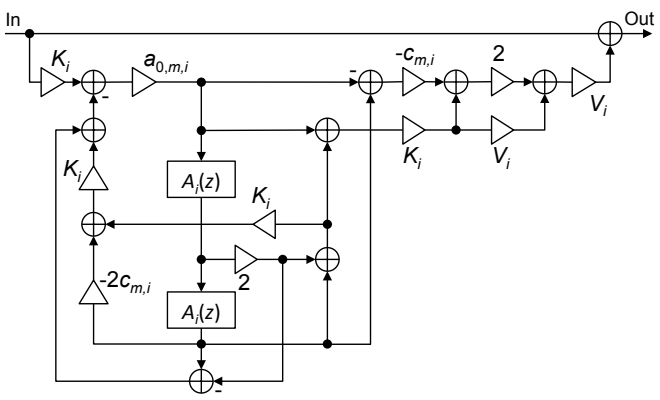

Fig. 2. The m^{th} fourth-order section of the i^{th} band filter [4], [15].

Fig. 1. The number of fourth-order sections utilized in a filter at band i is denoted by P_i, where $i = 1, 2, 3, ..., L$. The order of each band filter is $N_i = 4P_i$, since the filters have P_i fourth-order sections[1].

Fig. 2 shows the block diagram of the m^{th} fourth-order section of the high-order equalizer, where $c_{m,i} = \cos(\alpha_{m,i})$,

$$\alpha_{m,i} = \Big(\frac{1}{2} - \frac{2m-1}{4P_i}\Big)\pi, \tag{1}$$

and $m = 1, 2, \ldots, P_i$. Furthermore,

$$V_i = \sqrt[2P_i]{g_i} - 1, \tag{2}$$

$$K_i = \frac{1}{\sqrt[4P_i]{g_i}} \tan\Big(\frac{\Omega_{\mathrm{B},i}}{2}\Big), \tag{3}$$

and

$$a_{0,m,i} = 1 + 2K_i c_{m,i} + K_i^2, \tag{4}$$

where g_i is the desired gain in the i^{th} band and $\Omega_{\mathrm{B},i}$ is the normalized filter bandwidth [4]. $A_i(z)$ is a second-order allpass filter having the transfer function

$$A_i(z) = z^{-1}\frac{a_i + z^{-1}}{1 + a_i z^{-1}}, \tag{5}$$

where $a_i = \cos(\Omega_{\mathrm{M},i})$ and $\Omega_{\mathrm{M},i}$ is the optimized and normalized center frequency

$$\Omega_{\mathrm{M},i} = 2\arctan\sqrt{\tan(\frac{\Omega_{\mathrm{U},i}}{2})\tan(\frac{\Omega_{\mathrm{L},i}}{2})}, \tag{6}$$

where $\Omega_{\mathrm{U},i}$ and $\Omega_{\mathrm{L},i}$ are the normalized upper and lower cutoff frequency of the filter, respectively [4].

When the user of the graphic equalizer modifies the gain g_i of band i, parameters V_i, K_i, and $a_{0,m,i}$ must be recomputed using (2), (3), and (4), respectively, in all fourth-order sections of that band.

III. Optimizing Band Filter Orders

Fig. 3 illustrates the interaction at a transition band of two adjacent filters. The two bands used in this example are $i = 3$ and $i = 4$ (the bands correspond to bands 3 and 4 shown in Table I), where the filter in band 4 stays untouched while the order of the band 3 filter is altered. The filter in band 4 is shown in Fig. 3(a). The center frequency of band 4 is 350 Hz, the bandwidth is 100 Hz, the gain is -20 dB, and the order is eight. Thus it consists of two cascaded fourth-order sections as shown in Fig. 2.

[1]Note that the relationship between P and M is that the notation M used in previous publications [4], [18], [15], is $P_i = M/2$.

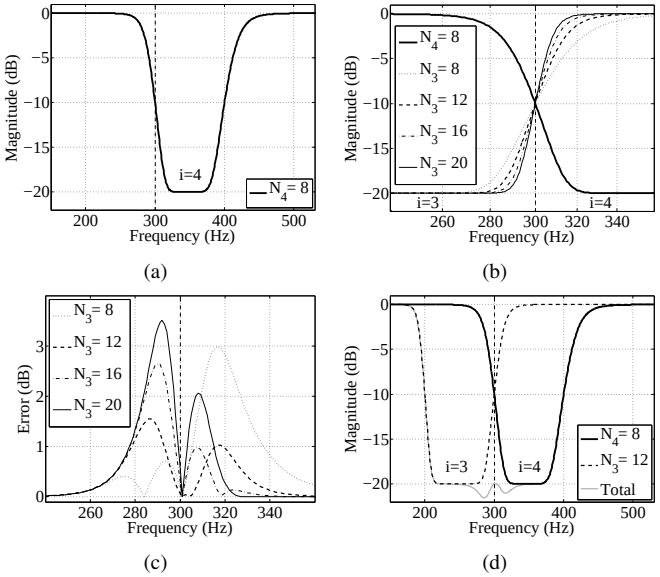

Fig. 3. Example of the interaction around the transition band of two adjacent band filters: (a) the magnitude response of the band 4 filter, (b) the same band 4 filter as well as four candidate filters for the adjacent band with different orders, (c) the absolute error around the transition band between bands 3 and 4, and (d) the magnitude response of the best matching filter along with the original band 4 filter and their combined response (gray curve).

Fig. 3(b) focuses on the lower transition band of band 4 and plots the responses of four candidate filters in the adjacent band ($i = 3$) of orders 8, 12, 16, and 20. The center frequency of band 3 is 250 Hz, the bandwidth is 100 Hz, and the gain is -20 dB. The thick black curve is a part of the same curve shown in Fig. 3(a). As can be seen in Fig. 3(b), the shape of the band 3 filter slope changes as the filter order is increased.

Fig. 3(c) shows the absolute error between the different orders of the filters in band 3 and the filter in band 4 when both their gain are set to -20 dB and the target curve lies at -20 dB. As can be seen in Fig. 3(c), the twelfth-order filter has the smallest peak error, approximately 1.5 dB. Furthermore, when the order is increased to 16 (or more), the peak error increases. Thus, an optimal solution for the filter order exists in terms of the peak error.

Finally, Fig. 3(d) shows the magnitude response of the twelfth-order filter in band 3 and the eight-order filter in band 4 side by side. Furthermore, the gray curve shows the total magnitude response of these two filters. The total magnitude response shows the effect of the imperfect transition band (around 300 Hz) as deviations from the target gain $G_{\text{target}} = -20$ dB.

Thus, by increasing the equalizer order at low and high frequencies, the error due to the interaction of the transition bands can be reduced until the minimum is reached. The main idea in optimizing the filter orders is to match the slopes of the adjacent filters so that the maximum error is within a set limit.

The maximum error in a transition band between the bands $i-1$ and i is

$$E_{\max,i-1} = \max_{\Omega_{\mathrm{M},i-1} \le \omega \le \Omega_{\mathrm{M},i}} \left\{ 20\log_{10}\left(|H_i(e^{j\omega}) H_{i-1}(e^{j\omega})| \right) - G_{\mathrm{target}} \right\}, \tag{7}$$

where $H_i(\omega)$ is the frequency response of the filter in the i^{th} band.

A. Algorithm

The inputs of the algorithm are the target gain G_{target} and the error tolerance E_δ in decibels, the start band i_{start}, and the maximum allowed number of fourth-order sections $P_{\max}$. The lower bands are optimized first ($i \le i_{\mathrm{start}}$) after which the higher bands ($i > i_{\mathrm{start}}$) are similarly optimized. The start band i_{start} should be in the frequency range where filters with same orders interact well, i.e., produce small error. The number of fourth-order sections is initially $P_i = 1$ for all bands i. The proposed iterative algorithm for bands where $i < i_{\mathrm{start}}$ operates as follows:

1) The combined magnitude response of two adjacent filters $H_i(z)$ and $H_{i-1}(z)$ is calculated while their gain is set to $g_i = g_{i-1} = G_{\mathrm{target}}$.
2) The response under observation is limited between the center frequencies $\Omega_{\mathrm{M},i}$ and $\Omega_{\mathrm{M},i-1}$ of the adjacent frequency bands, since the maximum error $E_{\max,i-1}$ is located around the transition band.
3) $E_{\max,i-1}$ around the transition band is calculated using (7). If this is the first round of iteration, i.e., the bands under observation are i_{start} and $i_{\mathrm{start}} - 1$, go to step 4, otherwise, go to step 5.
4) If $E_{\max,i-1} > E_\delta$, add one fourth-order block to both filters, i.e., increase P_i and P_{i-1} by one. Then start over from step 1.
   If $E_{\max,\mathrm{i}-1} \le E_\delta$, save the current values of P_i and P_{i-1}. Move on to optimizing the previous band by decrementing i by one and start over from step 1.
5) If $E_{\max,\mathrm{i}-1}$ in this iteration round is larger than that in the previous round, i.e., the error is increasing, save the previous number of fourth-order sections $P_{i-1} - 1$ and move on to optimizing the previous band by decrementing i by one and start over from step 1.
   If $E_{\max,\mathrm{i}-1} > E_\delta$, add one fourth-order block to the filter being optimized, i.e., increase P_{i-1} by one. Then start over from step 1.
   If $E_{\max,\mathrm{i}-1} \le E_\delta$, save the current number of fourth-order sections P_{i-1} and move on to optimizing the previous band by decrementing i by one and start over from step 1.

If $P_{\max}$ is reached at some point, the value of $P_{\max}$ becomes the optimized number of fourth-order sections for that band. The bands where $i > i_{\mathrm{start}}$ are optimized with the same logic, but $i-1$ is replaced with $i+1$ in steps 1, 2, and 5; step 4 is skipped; and i is increased by one instead of decreased by one in step 5.

The relevant Matlab code is available at http://www.acoustics.hut.fi/go/ieee-spl-hogeq.

TABLE I
FREQUENCY PARAMETERS (HZ) FOR BARK-BAND GRAPHIC EQUALIZER.

i	f_{L}	f_{U}	f_{B}	f_{M}	i	f_{L}	f_{U}	f_{B}	f_{M}
1	20	100	80	45	13	1720	2000	280	1855
2	100	200	100	141	14	2000	2320	320	2154
3	200	300	100	245	15	2320	2700	380	2503
4	300	400	100	346	16	2700	3150	450	2917
5	400	510	110	452	17	3150	3700	550	3415
6	510	630	120	567	18	3700	4400	700	4037
7	630	770	140	697	19	4400	5300	900	4833
8	770	920	150	842	20	5300	6400	1100	5830
9	920	1080	160	997	21	6400	7700	1300	7031
10	1080	1270	190	1171	22	7700	9500	1800	8579
11	1270	1480	210	1371	23	9500	12k	2500	10746
12	1480	1720	240	1596	24	12k	15.5k	3500	13842

IV. RESULTS

A. Design Example

We have previously utilized the recursive high-order graphic equalizer design to simulate the auditory masking phenomenon in headphone listening caused by background noise [15]. Since auditory masking is typically estimated using Bark bands, the high-order graphic equalizer was divided accordingly into Bark bands.

Table I shows the frequency parameters of the Bark-band graphic equalizer, where f_{L} is the lower cutoff frequency, f_{U} is the upper cutoff frequency, f_{B} is the bandwidth, and f_{M} is the optimized center frequency in Hertz, derived from the result of (6), i.e., $f_{\mathrm{M}} = f_{\mathrm{s}}\Omega_{\mathrm{M}}/(2\pi)$, where f_{s} is the sampling rate ($f_{\mathrm{s}} = 44100$ Hz). As can be seen from Table I, the frequency range is limited to 20–15500 Hz, since this range covers the majority of any audible audio content. Thus, the Bark graphic equalizer consists of 24 bands ($L = 24$).

Examination of the magnitude response reveals that the transition bands interact well with the same filter orders at middle frequencies, approximately from 500 Hz to 7 kHz. However, when moving towards lower or higher frequencies, the error due to the interaction at the transition bands increases.

The algorithm was observed to operate reliably when $i_{\mathrm{start}} = 9$, since the peak error between bands 8 and 9 is large enough compared to the other peak errors in the range where filters with the same order interact well (see Fig. 4(a)). If i_{start} is, e.g., 13, the first round of the iterative algorithm presented in Section III-A might result in smaller orders for bands 12 and 13 than is required for bands 8 and 9 to meet the error tolerance E_δ. Thus, the proposed optimization algorithm is semi-automatic in the sense that it requires user interaction in the initialization.

B. Comparison

Fig. 4 illustrates the magnitude response of the high-order Bark-band graphic equalizer described in Section IV-A when the target gain $G_{\mathrm{target}} = -20$ dB. This unusual specification is used to reveal the interaction between the neighboring band filters, and the benefit of the proposed optimization algorithm also becomes obvious by inspecting this example. Fig. 4(a) shows the magnitude response of a Bark-band equalizer, where

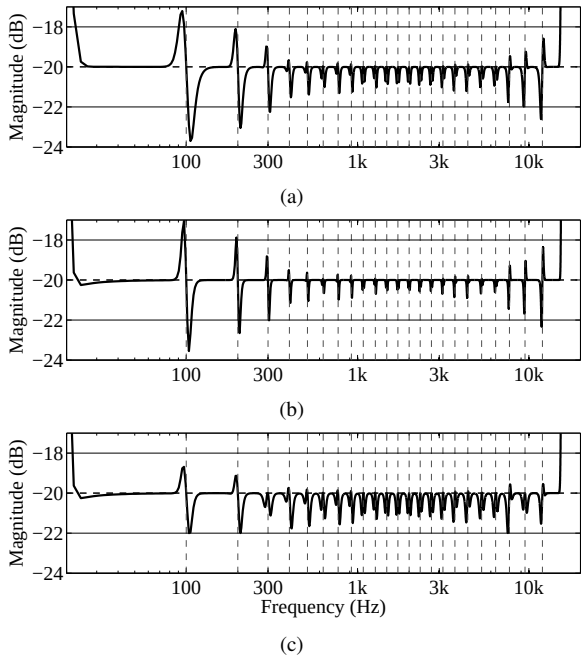

Fig. 4. Comparison of the magnitude responses of different Bark-band graphic equalizer filter orders, where (a) and (b) are the responses of non-optimized graphic equalizers with orders $N = 384$ and $N = 672$, respectively, and (c) is the response of the equalizer optimized with the proposed algorithm ($N = 328$). The solid horizontal lines indicate the ± 2 dB tolerances. The target gain is -20 dB in the frequency range of interest.

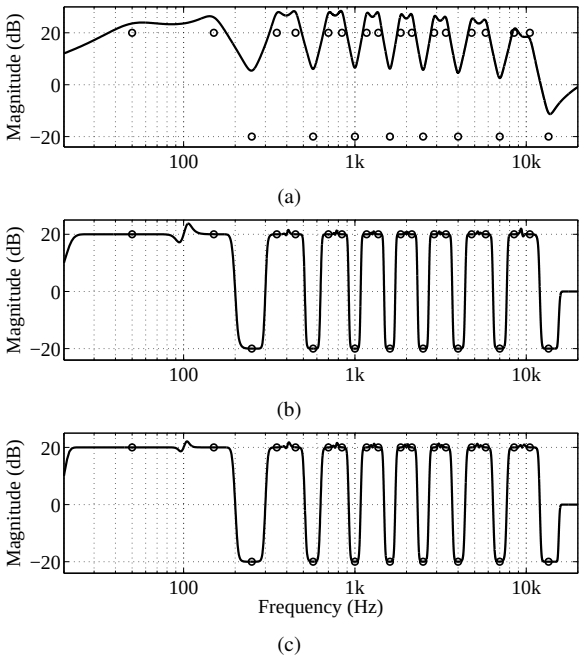

Fig. 5. Magnitude response of (a) a second-order Regalia-Mitra ($N = 48$), (b) a non-optimized ($N = 384$), and (c) an optimized graphic equalizer ($N = 328$). The circles indicate the command points of the graphic equalizer.

all the bands are of order 16, whereas in Fig. 4(b) every band has an order of 28, resulting in a total order of $N = 384$ and $N = 672$, respectively. In other words, the orders of neither of these designs are optimized, whereas the design producing the response presented in Fig. 4(c) is optimized using the algorithm presented in Section III-A.

The inputs of the algorithm were as follows: $G_{\mathrm{target}} = -20\,\mathrm{dB}$, $E_\delta = 2\,\mathrm{dB}$, and $i_{\mathrm{start}} = 9$. Furthermore, $P_{\max} = 20$ was large enough so as not to limit the operation of the algorithm. Starting from the first Bark band, the first three optimized orders are 28, 20, and 16; bands from 4 to 22 have the order 12; and the last two bands have the orders 16 and 20, respectively. Thus, the resulting total order is $N = 328$.

As can be seen in Fig. 4, the maximum peak error in Fig. 4(c) is within the ± 2 dB error range as specified, whereas in Figs. 4(a) and 4(b) the maximum peak error exceeds the specified maximum error, even though the total order of the equalizers is larger than the total order of the optimized equalizer in both cases.

Fig. 5 shows another example in Bark bands, where the circles illustrate the commands, i.e., the slider positions of the graphic equalizer, which are set to an extreme configuration so that every third command is at $-20\,\mathrm{dB}$ and the rest are at $20\,\mathrm{dB}$. This leads to a 40-dB gain difference between some neighboring bands as well as narrow flat regions both of which are known to be difficult challenges for a graphic equalizer.

Fig. 5(a) shows the magnitude response of a traditional graphical equalizer consisting of second-order Regalia-Mitra filters, which does not hit the commands. The bandwidths of the band filters are half of the nominal Bark bandwidths, since this choice provides generally a good performance. It would be possible to further improve the performance by optimizing both the gains and the bandwidths for the given commands [5]. However, it would not be comparable to the proposed design.

Figs. 5(b) and 5(c) show the magnitude response of the non-optimized and optimized high-order graphic equalizer, respectively. The non-optimized graphic equalizer consists of 16^{th}-order band filters like the one producing the response in Fig. 4(a). As can be seen in Fig. 5(c), the optimized graphic equalizer ($N = 328$) has the smallest frequency response deviations, even though it has a 15% smaller total order than the non-optimized equalizer ($N = 384$).

V. Conclusion

This letter examined the interaction of adjacent transition bands in a high-order graphic equalizer, which led to a novel algorithm for optimizing the band filter orders of the equalizer in order to minimize the peak error at the transition bands. By changing the filter order, the slope of the transition band changes, which makes it possible to decrease errors at the transition bands. The proposed semi-automatic optimization algorithm is started from a band filter in the middle frequencies, and then it proceeds automatically towards low and high frequencies, thus optimizing the order of all band filters of the graphic equalizer. The optimized graphic equalizer was shown to achieve smaller peak errors with lower total filter order than non-optimized graphic equalizers. Thus, the optimization algorithm enables the implementation of a precise and yet computationally efficient graphic equalizer.

REFERENCES

[1] P. Regalia and S. Mitra, "Tunable digital frequency response equalization filters," *IEEE Trans. Acoustics, Speech, and Signal Process.*, vol. 35, no. 1, pp. 118–120, Jan. 1987.

[2] T. van Waterschoot and M. Moonen, "A pole-zero placement technique for designing second-order IIR parametric equalizer filters," *IEEE Trans. Audio, Speech Lang. Process.*, vol. 15, no. 8, pp. 2561–2565, Nov. 2007.

[3] J. D. Reiss, "Design of audio parametric equalizer filters directly in the digital domain," *IEEE Trans. Audio, Speech Lang. Process.*, vol. 19, no. 6, pp. 1843–1848, Aug. 2011.

[4] M. Holters and U. Zölzer, "Graphic equalizer design using higher-order recursive filters," in *Proc. Int. Conf. Digital Audio Effects (DAFx-06)*, Sept. 2006, pp. 37–40.

[5] S. Tassart, "Graphical equalization using interpolated filter banks," *J. Audio Eng. Soc.*, vol. 61, no. 5, pp. 263–279, May 2013.

[6] S. Särkkä and A. Huovilainen, "Accurate discretization of analog audio filters with application to parametric equalizer design," *IEEE Trans. Audio, Speech Lang. Process.*, vol. 19, no. 8, pp. 2486–2493, Nov. 2011.

[7] S. K. Mitra, *Digital Signal Processing: A Computer Based Approach*, 3rd ed. McGraw-Hill, New York, 2006.

[8] H. Behrends, A. von dem Knesebeck, W. Bradinal, P. Neumann, and U. Zölzer, "Automatic equalization using parametric IIR filters," *J. Audio Eng. Soc.*, vol. 59, no. 3, pp. 102–109, Mar. 2011.

[9] R. Ansari, "Multi-level IIR digital filter," *IEEE Trans. Circ. Syst.*, vol. 33, no. 3, pp. 337–341, Mar. 1986.

[10] S. Cecchi, L. Palestini, E. Moretti, and F. Piazza, "A new approach to digital audio equalization," in *Proc. IEEE Workshop on Applications of Signal Processing to Audio and Acoustics*, New Paltz, NY, Oct. 2007, pp. 62–65.

[11] R. Väänänen and J. Hiipakka, "Efficient audio equalization using multirate processing," *J. Audio Eng. Soc.*, vol. 56, no. 4, pp. 255–266, Apr. 2008.

[12] U. Zölzer and T. Boltze, "Parametric digital filter structures," in *Proc. AES 99th Convention*, New York, NY, Oct. 1995.

[13] F. Fontana and M. Karjalainen, "A digital bandpass/bandstop complementary equalization filter with independent tuning characteristics," *IEEE Signal Process. Lett.*, vol. 10, no. 4, pp. 119–112, Apr. 2003.

[14] S. K. Mitra, "LTI discrete-time systems in the transform domain," in *Digital Signal Processing: A Computer Based Approach*. 3rd ed., New York, McGraw-Hill, 2006, ch. 7, sec. 7.1.1, pp. 353–355.

[15] J. Rämö, V. Välimäki, M. Alanko, and M. Tikander, "Perceptual frequency response simulator for music in noisy environments," in *Proc. AES 45th Int. Conf.*, Helsinki, Finland, Mar. 2012.

[16] J. Rämö, V. Välimäki, and M. Tikander, "Perceptual headphone equalization for mitigation of ambient noise," in *Proc. IEEE Int. Conf. Acoustics, Speech, and Signal Processing*, Vancouver, Canada, May 2013, pp. 724–728.

[17] S. J. Orfanidis, "High-order digital parametric equalizer design," *J. Audio Eng. Soc.*, vol. 53, no. 11, pp. 1026–1046, Nov. 2005.

[18] M. Holters and U. Zölzer, "Parametric recursive high-order shelving filters," in *Proc. AES 120th Convention*, Paris, France, May 2006.